Nonparabolicity effects on electron–optical-phonon scattering rates in quantum wells

Augusto M. Alcalde
Instituto de Física, Universidade Estadual de Campinas, Caixa Postal 6165, 13083-970 Campinas SP, Brazil

Gerald Weber
Departamento de Física Geral e Aplicada, Universidade São Francisco, 13251-900 Itatiba SP, Brazil

(Received 12 February 1997)

The scattering rates for intrasubband and intersubband transitions due to electron–optical-phonon interaction are calculated for GaAs-$Al_xGa_{1-x}As$ quantum wells taking into account the conduction subband nonparabolicity. For the description of the confined- and interface-phonon modes we use a dielectric continuum model and the nonparabolic conduction-subband energy is introduced as a second order expansion of k^2, the square of the electron wave vector. Our results show that for transitions due to the emission of confined phonons the scattering rates are significantly increased, while for interface phonons the scattering rates are decreased. In particular, we show that for high kinetic energies electrons will relax at an almost constant rates for quantum wells larger than 120 Å. We show that our results can be understood in terms of the phonon wave vector (or Fröhlich electron-phonon coupling), the density of final states, and the electron-phonon overlap. [S0163-1829(97)05336-8]

I. INTRODUCTION

Electron-phonon interaction in polar semiconductor quantum wells attracted a great amount of interest over the past years due to its importance for electronic properties. For instance, the cooling of photoexcited carriers, carrier tunneling, and the mobility of high-speed heterostructure devices are primarily governed by the scattering of electrons by polar-optical-phonons. Particular interest was directed towards optical phonon confinement effects (i.e., confined and interface-phonon modes) which affects significantly the scattering rates in quantum wells.

The electron–optical-phonon interaction in quantum wells was studied using either dielectric continuum models[1–3] or microscopic lattice dynamical models,[4–6] and much emphasis was given on the influence of the specific phonon model employed. In general, the use of dielectric continuum models is well established[5] and scattering rates calculated with such models compare successfully with experimental results.[7–9] From the calculation of capture times[10] it became evident that capture processes with large kinetic energy influence the overall capture time. For those large kinetic energies, implying in large momenta, the parabolic-band approximation becomes less justified even for GaAs-$Al_xGa_{1-x}As$ structures where in general nonparabolicity effects can be safely neglected. A question which has not yet been properly addressed is how strongly the subband nonparabolicity affects the intra- and intersubband scattering rates in quantum wells.

In this paper, we investigate systematically the influence of band nonparabolicity on the intra- and intersubband scattering rates due to emission of confined phonons and interface phonons. Also, we consider the case of transitions taking place at high kinetic energies. In a previous paper we reported some results on confined modes with low electron kinetic energy.[11] Our main purpose is to determine the importance of the subband nonparabolicity on the scattering rates and to identify the physical origin of the changes introduced by this nonparabolicity. Our results are always compared with scattering rates in the parabolic-subband approximation in order to determine exactly where and why quantitative and qualitative differences occur. Furthermore, the theory developed in this work can be used easily to include nonparabolic subbands in existing theoretical frameworks, which use dielectric continuum models for the calculation of scattering rates.

This paper is organized as follows: the general formal theory of the electron-phonon interaction and the scattering rates calculation is discussed in Sec. II A; Sec. II B describes briefly the electron envelope function used in this paper. In Sec. III we present and discuss our results. Finally, in Sec. IV we present our conclusions.

II. THEORY

A. Transition rates

The scattering rate of an electron from an initial state $|\mathbf{K}_i\rangle$ to a final state $|\mathbf{K}_f\rangle$ accompanied by the emission or absorption of a phonon with energy $\hbar\omega$ is given by the Fermi golden rule

$$W^{(l)}=\frac{2\pi}{\hbar}\int \delta(\mathcal{E}_i-\mathcal{E}_f\pm\hbar\omega)|\langle\mathbf{K}_f|H_{e\text{-ph}}|K_i\rangle|^2 dN_f, \quad (1)$$

where $\mathcal{E}$ is the total electron energy and $H_{e\text{-ph}}$ represents the electron-phonon interaction Hamiltonian. In this expression the integration is over the number of final states N_f. In order to take into account the different effective masses of the barrier and the well, we express our results as an average scattering rate $W=p_W W^{(W)}+p_B W^{(B)}$, where p_W (p_B) is the probability of finding the electron initially in the well (barrier) subband. In order to ease the notation we will drop the index $l=W,B$ (well or barrier, respectively), which refers to the effective mass mismatch.[12]

In order to introduce the subband nonparabolicity we start from an expression for the bulk conduction-band dispersion expanded up to second order in k^2, obtained from the Kane model

$$\mathcal{E}-V=\frac{\hbar^2k^2}{2m^*}(1-\gamma k^2), \tag{2}$$

where m^* is the band edge mass and γ the nonparabolicity parameter. V is the bulk conduction-band offset taken as $V=0$ in the well and $V=V_0$ in the barrier. The central problem of introducing such a nonparabolic energy dispersion relies in the δ function of the Fermi golden rule. This δ function represents the energy conservation and is written, for phonon emission, as

$$\delta(\mathcal{E}_i-\mathcal{E}_f-\hbar\omega)=\delta[f(\cos\theta)]=\delta(a\cos^2\theta+b\cos\theta+c), \tag{3}$$

where $\cos\theta$ is related to the in-plane momentum conservation for the emission of a phonon with momentum $q_\parallel$,

$$k_{\parallel f}^2=k_{\parallel i}^2+q_\parallel^2-2k_{\parallel i}q_\parallel\cos\theta, \tag{4}$$

and a, b, and c are defined as

$$a=\frac{\hbar^2}{2m^*}4\gamma k_{\parallel i}^2q_\parallel^2, \tag{5a}$$

$$b=\frac{\hbar^2}{2m^*}[2k_{\parallel i}q_\parallel-4\gamma(k_{\parallel i}^2+q_\parallel^2)k_{\parallel i}q_\parallel-4\gamma k_{zf}^2k_{\parallel i}q_\parallel], \tag{5b}$$

$$c=\frac{\hbar^2}{2m^*}\{k_{\parallel i}^2[1-\gamma(k_{\parallel i}^2+2k_{zi}^2)]-(k_{\parallel i}^2+q_\parallel^2)(1-2\gamma k_{zf}^2)+\gamma(k_{\parallel i}^2+q_\parallel^2)^2+Q^2\}, \tag{5c}$$

and for phonon emission Q is given by

$$Q^2=\pm\frac{2m^*}{\hbar^2}(E_i-E_f-\hbar\omega_{\mathrm{LO}}), \tag{6}$$

where the upper sign corresponds to intrasubband transitions and the lower sign corresponds to intersubband transitions, $E=\mathcal{E}(k_\parallel=0)$ are the confined energy levels and k_z is the z component of the initial (final) electronic wave vector for intrasubband (intersubband) transitions. Using basic δ function properties and making $x=\cos\theta$, we obtain

$$\delta(\mathcal{E}_i-\mathcal{E}_f-\hbar\omega)=\delta[f(x)]=|b^2-4ac|^{-1/2}\delta(x-R_-), \tag{7}$$

where R_- is the negative root of $f(x)=0$. The positive root R_+ is neglected because it diverges in the limit $\gamma\to0$.

The electron-confined LO-phonon interaction Hamiltonian in heterostructures as derived from Fröhlich interaction is given by[13,14]

$$H_n=\frac{\lambda}{\sqrt{V}}\sum_{q_\parallel}\exp(i\mathbf{q}_\parallel\cdot\mathbf{r}_\parallel)t_n(q_\parallel)u_{\parallel n}(z)[a_n(\mathbf{q}_\parallel)+a_n^\dagger(-\mathbf{q}_\parallel)], \tag{8}$$

where a_n and $a_n^\dagger$ are the phonon annihilation and creation operators, respectively, and

$$\lambda^2=4\pi e^2\hbar\omega_{\mathrm{LO}}(\epsilon_\infty^{-1}-\epsilon_s^{-1}), \tag{9}$$

where ϵ_s and ϵ_∞ are, respectively, the static and high-frequency dielectric constants, ω_{LO} is the LO-phonon frequency, e is the electron charge, and $\mathbf{q}_\parallel$ and $\mathbf{r}_\parallel$ are the parallel components of the phonon wave vector and position vector, respectively.

The normalization of the phonon displacement is $t_n(q_\parallel)=(2I_n)^{-1/2}$ with

$$I_n=\frac{1}{L}\int_{-L/2}^{+L/2}\left[q_\parallel^2u_n^2+\left(\frac{du_n}{dz}\right)^2\right]dz, \tag{10}$$

and for most dielectric continuum models[1–3] $t_n(q_\parallel)$ can be written in a general form

$$t_n(q_\parallel)=(a_nq_\parallel^2+b_n/L^2), \tag{11}$$

where the coefficients a_n and b_n are specific to each phonon model.

The scattering rate for confined modes is given by

$$W=\frac{\lambda^2}{\pi\hbar L}\sum_n|G_n|^2(N_{\mathbf{q}}+1)\times\int_{q_\parallel^-}^{q_\parallel^+}t_n^{-1}(q_\parallel)|b^2-4ac|^{-1/2}(1-R_-^2)^{-1/2}q_\parallel dq_\parallel, \tag{12}$$

where $N_{\mathbf{q}}$ is the phonon ocupation number and G_n is the overlap integral of the electron wave function and the z-dependent part of the electron-confined-phonon Hamiltonian,

$$G_n=\int_{-L/2}^{+L/2}\psi_f^*(z)u_{\parallel n}(z)\psi_i(z)dz. \tag{13}$$

The lower $q_\parallel^-$ and upper $q_\parallel^+$ integration limits of Eq. (12) are given as

$$q_\parallel^\pm=k_{\parallel i}\pm\sqrt{\mathcal{K}}, \tag{14}$$

where

$$\mathcal{K}=\frac{(1-2\gamma k_{zf}^2)-\{(1-2\gamma k_{zf}^2)^2-4\gamma[k_{\parallel i}^2(1-\gamma k_{\parallel i}^2)-2\gamma k_{\parallel i}^2k_{zi}^2+Q^2]\}^{1/2}}{2\gamma}. \tag{15}$$

The integral in Eq. (12) is valid for any initial or final electron energy, but it has to be evaluated numerically. However, this integral can be evaluated exactly in the limit case where for intrasubband transitions the electron has just enough energy to emit one LO confined-phonon ($k_{\|f}=0$) and for intersubband transitions where the electron is initially at the bottom of the subband ($k_{\|i}=0$).

$$W=\frac{m^*\lambda^2 L}{\hbar^3}\sum_n |G_n|^2(N_{\mathbf{q}}+1)\frac{1}{\alpha} \times\left\{\frac{a_n L^2}{2\gamma}[(1-2\gamma k_z^2)-\alpha]+b_n\right\}^{-1}, \tag{16}$$

where

$$\alpha=[(2\gamma k_z^2-1)^2+4\gamma Q^2]^{1/2}, \tag{17}$$

where $k_z=k_{zi}$ and $k_z=k_{zf}$ are for intra- and intersubband transitions, respectively.

Note that Eq. (16) has a nontrivial limit for $\gamma\to 0$. But an elementary application of L'Hopital rule shows that in this limit (16) becomes the well-known scattering rates for parabolic subbands,[1,2]

$$W=\frac{m^*\lambda^2 L}{\hbar^3}\sum_n |G_n^{i\to f}|^2(N_{\mathbf{q}}+1)[\mp Q^2 a_n L^2+b_n]^{-1}. \tag{18}$$

An important characteristic of the scattering rates in Eqs. (12) and (16) is that they follow exclusively from the energy dispersion relation, Eq. (2). No additional assumption about the confined-phonon model nor the method which calculates the energy eigenvalues and eigenfunctions was made. In this work we use the reformulated[15] slab model for which t_n is given by

$$t_n(q_\|)=\begin{cases}[q_\|^2+(n+1)^2\pi^2/L^2]^{-1/2}, & n=1,3,5,\ldots\\ [3q_\|^2+n^2\pi^2/L^2]^{-1/2}, & n=2,4,6,\ldots\ .\end{cases} \tag{19}$$

For the description of the electron-interface-phonon interaction we use the Hamiltonian proposed by Mori and Ando.[14] The electron-phonon Hamiltonian for interface phonon in heterostructures is given by

$$H_{\nu\mu}=\sum_{q_\|}\left(\frac{\hbar\omega_{\nu\mu}e^2}{2\epsilon_0 L^2}\right)^{1/2} f_{\nu\mu}(q_\|)h_\nu(q_\|,z) \times\frac{e^{i\mathbf{q}_\|\cdot\mathbf{r}_\|}}{\sqrt{2q_\|}}[a_{\nu\mu}(\mathbf{q}_\|)+a_{\nu\mu}^\dagger(-\mathbf{q}_\|)], \tag{20}$$

where $\omega_{\nu\mu}$ is the interface-phonon frequency, ϵ_0 is the permitivity of vacuum, and $a_{\nu\mu}$ and $a_{\nu\mu}^\dagger$ are the interface-phonon annihilation and creation operators, respectively. The subscript ν refers to the parity (symmetric or antisymmetric) and μ the possible solution of the interface-phonon dispersion equations (GaAs and AlAs-like modes). For additional details and definitions of the remaining parameters of the electron-phonon Hamiltonian we refer the reader to the work of Mori and Ando.[14]

For interface modes, we can write the final general form of the nonparabolic scattering rates as

$$W=\frac{e^2}{4\pi\epsilon_0}(N_{\mathbf{q}}+1)\int_{q_{\|\min}}^{q_{\|\max}}\omega_{\nu\mu}(q_\|) \times|b^2-4ac|^{-1/2}f_{\nu\mu}^2(q_\|)|G_{\nu\mu}(q_\|)|^2(1-R_-)^{-2}dq_\|. \tag{21}$$

The integration limits $q_{\|\max}$ and $q_{\|\min}$ are obtained numerically by taking into account the interface-phonon dispersion, the in-plane momentum conservation, and the energy conservation.

Similar as for confined-phonon modes, we obtain an analytic expression for intrasubband transitions where the electron has just enough energy to emit one LO confined-phonon ($k_{\|f}=0$) and for intersubband transitions where the electron is initially at the bottom of the subband ($k_{\|i}=0$),

$$W=\frac{\omega_{\nu\mu}(q_\|)e^2m^*}{4\hbar^2\epsilon_0}(N_{\mathbf{q}}+1)\frac{1}{\alpha}\frac{|G_{\nu\mu}(P)|^2f_{\nu\mu}^2(P)}{P}, \tag{22}$$

where

$$P^2=\frac{(1-2k_z^2\gamma)-\alpha}{2\gamma}, \tag{23}$$

and α is functionally defined by Eq. (17) and k_z is the z component of the initial (final) electronic wave vector for intrasubband (intersubband) transitions. In this work we are taking into account the interface-phonon dispersion, using the appropriate values of $\omega_{\nu\mu}$ and $q_\|$ which are calculated for each given electron energies.

The overlap of the electron wave function and the z-dependent part of the electron-interface-phonon Hamiltonian is given by

$$G_{\nu\mu}=\int_{-\infty}^{+\infty}\psi_f^*(z)h_\nu(q_\|,z)\psi_i(z)dz. \tag{24}$$

B. Envelope functions

For the description of the electron subband nonparabolicity, several models were proposed, e.g., Refs. 16–19, where the main differences between those models are the form of the energy dispersion relation describing the subband nonparabolicity and the definition of appropriate energy effective masses. The effective mass enters in the analysis when the wave vector is evaluated for a given energy and also when the derivatives of the envelope functions are matched at the heterojunction interface.

The question of energy dependent effective masses is at present the subject of some controversy; a particular aspect of this problem consists in the definition of the parallel component of the effective mass, the concept of which has been treated in the literature for superlattices[20] and quantum wells.[17,21,22] In our specific calculation, the application of this description is not immediate, since the dispersion relation given by the Eq. (2) cannot be expressed like the sum of parallel $\mathcal{E}(k_\|)$ and perpendicular $\mathcal{E}(k_z)$ components. This typical characteristic of nonparabolic structure in finite quantum wells is due to coupling between $k_\|$ and k_z through of

nonparabolic parameter γ. In order to estimate the effect of a heavier parallel mass, we included in Eq. (5c) a definition of parallel masses, given in Refs. 17,21, in the isotropic limits. For narrow quantum wells (50–70 Å) in both intra- and intersubband, the maximum increase of the order of 4% is obtained. This effect is significatively reduced when the quantum well width is increased. In all cases tested, the inclusion of this parallel mass definition did not modify the behavior of the scattering.

For the theory outlined in Sec. II A one may use any model which describes the subband nonparabolicity in the form of Eq. (2). We follow the model proposed by Nag and Mukhopadhyay,[18] which was shown to adequately describe the energy levels with subband nonparabolicity in GaAs-$Al_xGa_{1-x}As$ quantum wells. This model writes the electron envelope wave function in the same functional form as for the simple parabolic subband model for a finite barrier quantum well,

$$\psi(z)=\begin{cases} A\exp(-k_B z), & z<-L/2 \\ B\sin(k_W z)+C\cos(k_W z), & |z|<L/2 \\ D\exp(k_B z), & z>L/2, \end{cases} \tag{25}$$

where, as usual, the constants A, B, C, and D are found by applying boundary conditions and by normalizing the wave function. The information about the subband nonparabolicity is contained in the energy-dependent definition of the effective masses. The only one difference compared to the parabolic case is that the relation between the parameters k_W and k_B and the energy are more complicated due to presence of energy effective masses. An immediate advantage of the functional form of Eq. (25) is that the overlap integrals, Eqs. (13) and (24), are functionally the same as in previous calculations.[1,2] Therefore, this model is particularly well suited for the comparative study of scattering rates for parabolic and nonparabolic electron subbands.

A drawback of this model is that the wave functions of the first and third state are not completely orthogonal. This nonorthogonality, which affects only the $3\rightarrow1$ transitions, is associated to the problematic definitions of energy dependent effective masses and boundary conditions, but does otherwise not affect the electron-phonon transition selection rules. We have numerically estimated that this nonorthogonality may cause a variation of the order of 1% in the overlap integrals of the $3\rightarrow1$ transitions and therefore has a negligible effect on the scattering rates.

III. RESULTS AND DISCUSSION

For the calculations of scattering rates due to emission of confined longitudinal-optical phonons we assume a GaAs-$Al_xGa_{1-x}As$ quantum well with finite barriers of 224 meV corresponding to $x=0.3$. The material parameters used in our calculations are[23] for GaAs, the effective mass $m_W^*=0.0665\,m_0$, the dielectric constants $\varepsilon_0=12.35$ and $\varepsilon_\infty=10.48$, the bulk phonon energies $\hbar\omega_{\rm LO}=36.8$ meV, and $\hbar\omega_{\rm TO}=33.29$ meV the nonparabolicity parameter is taken as[16,18] $\gamma_W=4.9\times10^{-19}$ m^2; for $Ga_xAl_{1-x}As$, the effective mass $m_B^*=0.0901m_0$, the dielectric constants $\varepsilon_0=14.12$ and $\varepsilon_\infty=10.07$, the phonon energies $\hbar\omega_{\rm LO}=46.97$ meV, and $\hbar\omega_{\rm TO}=44.77$ meV the nonparabolicity parameter $\gamma_B=2.67\times10^{-19}$ m^2. The phonon occupation number is assumed $N_{\mathbf{q}}\sim0$, which is valid for low temperatures.

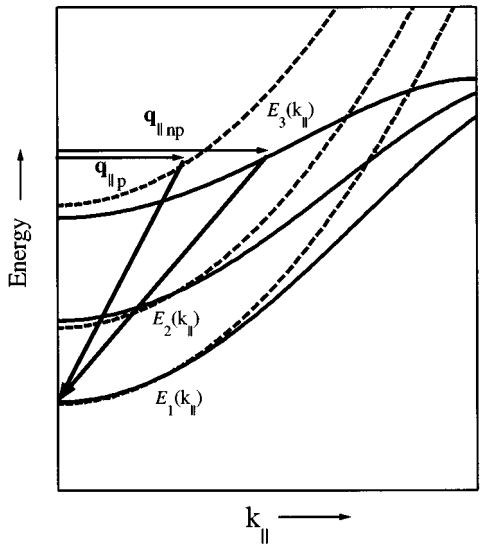

FIG. 1. Schematic diagram for intrasubband and intersubband transitions in quantum wells. The solid lines represent nonparabolic conduction subbands and the dashed lines are for parabolic subbands.

Before we present the results of our calculations, we will briefly discuss some aspects of the subband nonparabolicity which are expected to affect the scattering rates. In Fig. 1 we present a schematic diagram of phonon wave vectors which shows that for nonparabolic subbands the phonon wave vector is larger than for parabolic subbands. It is well known that the electron-phonon interaction has a strong dependence on these wave vectors, for the Fröhlich interaction which is roughly proportional to $1/q$ this indicates that the electron couples more weakly to the phonon for nonparabolic subbands. Therefore, these larger phonon wave vectors will reduce the scattering rates. Furthermore, one expects that the electron-phonon coupling will be more affected for transitions involving electrons with larger kinetic energies.

The Fermi golden rule depicted in Eq. (1) is an integral of matrix elements over final states, therefore the density of states plays a major role for scattering rates. Figure 2 shows the density of states for nonparabolic subbands described by Eq. (2),

$$g_{\rm np}=\frac{m^*}{\pi\hbar}\left(1+\frac{4m^*\gamma}{\hbar^2}\mathcal{E}\right), \tag{26}$$

and compares it with the density of states in the parabolic subband approximation for the first three subbands of a GaAs-$Al_{0.3}Ga_{0.7}As$ quantum well. Figure 2 illustrates clearly that although the energy levels do not change appreciably due to subband nonparabolicity, the density of states indeed do vary significantly. With a larger density of states within the energy range of a LO phonon one expects an increase of the scattering rates. One exception is intrasubband transitions with just enough initial kinetic energy to emit one phonon. In this case the final state of the electron is at the bottom of the subband ($k_{\parallel f}=0$) where the densities of states of the parabolic and nonparabolic subbands are the same. Thus, for

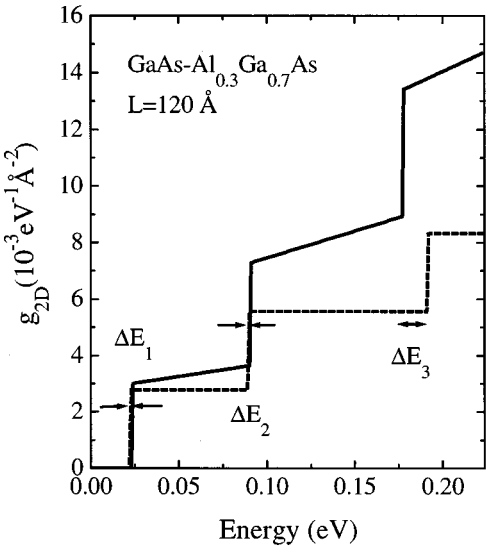

FIG. 2. Density of states calculated for a GaAs-$Al_{0.3}Ga_{0.7}As$ quantum well of width $L = 120$ Å, for parabolic (dashed line) and nonparabolic (solid line) electron subbands. ΔE_n represents the confined energy shift induced by the subband nonparabolicity.

these transitions the densities of final states neither enhance nor decrease the scattering rates.

The third key element which influences the scattering rates are the overlap integrals given by Eqs. (13) and (24). In general, the subband nonparabolicity electron wave function becomes more confined in the z direction, i.e., to the quantum well. Thus the confined phonon modes will have larger overlap integrals (increasing scattering rates) while the interface-phonon modes will present smaller overlap integrals (decreasing scattering rates). As we shall see, most results can be understood in terms of the phonon wave vector, the density of states, and the overlap integrals.

The scattering rates due to confined- and interface-phonon modes for $1 \rightarrow 1$ intrasubband transitions are shown in Fig. 3, where the initial electron energy is just enough to emit one phonon. The scattering rate due to confined modes become larger with the subband nonparabolicity and the rates due to

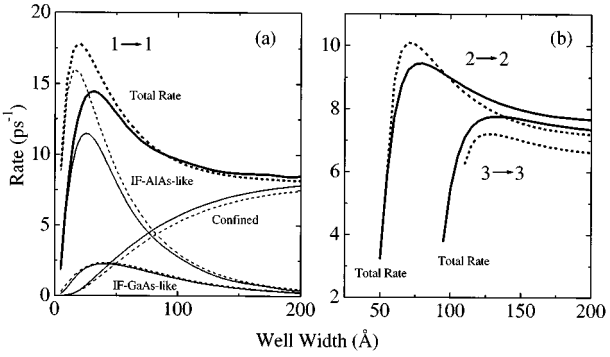

FIG. 3. Intrasubband transition rates as a function of the well width, due to confined- and interface-phonon modes. (a) Confined and GaAs-like and AlAs-like interface-phonon contributions to the total scattering rate for the $1 \rightarrow 1$ transition, (b) total scattering rates for $2 \rightarrow 2$ and $3 \rightarrow 3$ transitions. Solid and dashed lines are for nonparabolic and parabolic subbands, respectively.

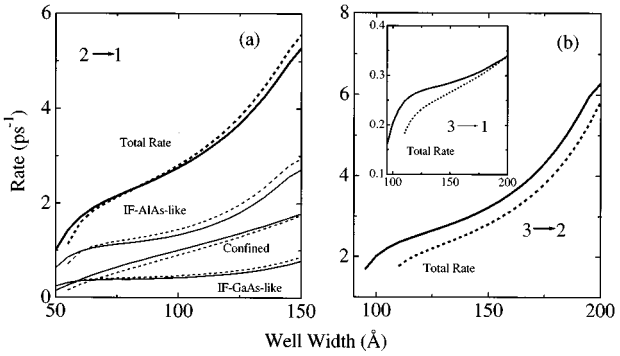

FIG. 4. Intersubband transition rates as a function of the well width, due to confined- and interface-phonon modes. (a) Confined and GaAs-like and AlAs-like interface-phonon contributions to the total scattering rate for the $2 \rightarrow 1$ transition, (b) total scattering rates for $3 \rightarrow 1$ and $3 \rightarrow 2$ transitions. Solid and dashed lines are for nonparabolic and parabolic subbands, respectively.

interface-phonon modes become smaller. The larger phonon wave vector reduces the scattering rates, and for these specific transitions the density of states does not affect the scattering rates. For confined modes, this decrease is compensated by larger overlap integrals and therefore these rates are generally larger for nonparabolic subbands. On the other hand, for interface modes both larger wave vectors and smaller overlap integrals are reducing the scattering rates quite significantly, especially for narrower quantum wells. The AlAs-like interface modes have larger phonon energies and thus wave vectors than GaAs-like modes, which explains the pronounced effect on AlAs-like modes. It is interesting to note that the total scattering rate (confined and both interface modes) also changes with the subband nonparabolicity, i.e., the increase of rates due to confined modes and the decrease due to interface modes do not compensate each other. This can be understood by the fact that these transitions have quite different phonon wave vectors and that the difference in the magnitude of these wave vectors is enhanced by the subband nonparabolicity. For intrasubband transitions involving higher subbands, see Fig. 3(b), the differences between the rates with parabolic and nonparabolic transitions are even more pronounced.

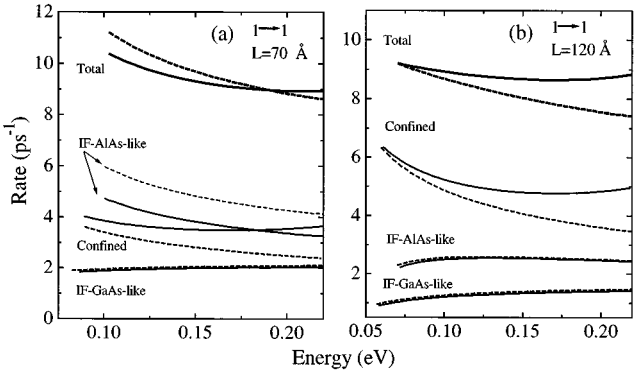

FIG. 5. Intrasubband transition rates as a function of electron energy, including GaAs-like and AlAs-like interface modes. Solid lines refer to the nonparabolic rates and dashed lines are parabolic calculations. A well width of 70 Å is assumed in part (a) and 120 Å in part (b).

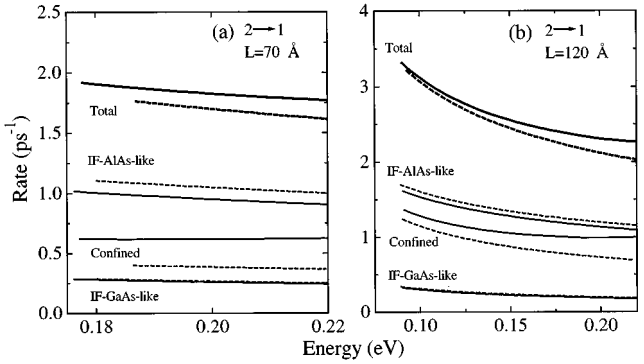

FIG. 6. Intersubband transition rates as a function of electron energy, including GaAs-like and AlAs-like interface modes. Solid lines refer to the nonparabolic rates and dashed lines are parabolic calculations. A well width of 70 Å is assumed in part (a) and 120 Å in part (b).

For intersubband transitions, the effect of subband nonparabolicity on the density of final states largely compensates the increase of phonon wave vectors leaving the scattering rates essentially unchanged. This is verified in Fig. 4 where we present the scattering rates of intersubband transitions where the initial state is at the bottom of the subband.

Scattering rates for electrons with higher initial energy are shown in Figs. 5 and 6 for several intra- and intersubband scattering rates, respectively. As expected, as we move into high energy regions of the electron subband the nonparabolicity effects become more pronounced. For intrasubband transitions, Fig. 5, the effect of the subband nonparabolicity is more important for narrow quantum wells than for larger wells. However, the most interesting aspect is that in some cases, e.g., confined modes for 120 Å quantum well [Fig. 5(b)], the scattering rates increase for higher kinetic energies. Indeed, the total scattering rate for $1\rightarrow1$ transitions for larger quantum wells remains almost constant for higher kinetic energy indicating that carrier relaxation will take place at a uniform rate.

IV. CONCLUSIONS

We have presented a systematic study of the electron subband nonparabolicity on intrasubband and intersubband scattering rates as due to confined- and interface-phonon emission. The theory presented can be applied to several dielectric continuum models and can be used together with any electron envelope function which describes the subband nonparabolicity as a second order expansion in k^2. We have shown that the effect of these subband nonparabolicity scattering rates can be understood in terms of the phonon wave vector, the density of final states, and the electron-phonon overlap. The case of electron relaxation at higher kinetic energies was also analyzed and we found that for quantum wells of the order of 120 Å, or larger, this relaxation occurs at an almost constant rate.

ACKNOWLEDGMENTS

We acknowledge financial support from Fapesp (96/5037-2, 95/9437-2) and CNPq (522789/96-0).

[1] S. Rudin and T. L. Reinecke, Phys. Rev. B **41**, 7713 (1990).
[2] G. Weber, A. M. de Paula, and J. F. Ryan, Semicond. Sci. Technol. **6**, 397 (1991).
[3] J. Shi and S. Pan, Phys. Rev. B **51**, 17 681 (1995).
[4] P. Lugli *et al.*, Semicond. Sci. Technol. **7**, B116 (1992).
[5] H. Rücker, E. Molinari, and P. Lugli, Phys. Rev. B **45**, 6747 (1992).
[6] A. R. Bhatt, K. W. Kim, M. A. Stroscio, and J. M. Higman, Phys. Rev. B **48**, 14 671 (1993).
[7] G. Weber and A. M. de Paula, Appl. Phys. Lett. **63**, 3026 (1993).
[8] A. M. de Paula and G. Weber, Appl. Phys. Lett. **65**, 1281 (1994).
[9] K. L. Schumacher, D. Collings, R. T. Phillips, D. A. Ritchie, G. Weber, J. N. Schulman, and K. Ploog, Semicond. Sci. Technol. **11**, 1173 (1996).
[10] A. M. de Paula and G. Weber, J. Appl. Phys. **77**, 6306 (1995).
[11] A. M. Alcalde and G. Weber, Solid State Commun. **96**, 763 (1995).
[12] G. Bastard, *Wave Mechanics Applied to Semiconductor Heterostrucures* (Les Editions de Physique, Les Ulis, France, 1988).
[13] J. J. Licari and R. Evrard, Phys. Rev. B **15**, 2254 (1977).
[14] N. Mori and T. Ando, Phys. Rev. B **40**, 6175 (1989).
[15] G. Weber, Phys. Rev. B **46**, 16 171 (1992).
[16] D. F. Nelson, R. C. Miller, and D. A. Kleinman, Phys. Rev. B **35**, 7770 (1987).
[17] U. Ekenberg, Phys. Rev. B **36**, 6152 (1987).
[18] B. R. Nag and S. Mukhopadhyay, Phys. Status Solidi B **175**, 103 (1993).
[19] B. R. Nag, Appl. Phys. Lett. **59**, 1620 (1991).
[20] G. Bastard, Phys. Rev. B **25**, 7584 (1982).
[21] U. Ekenberg, Phys. Rev. B **40**, 7714 (1989).
[22] B. R. Nag and S. Mukhopadhyay, Appl. Phys. Lett. **62**, 2416 (1993).
[23] S. Adachi, J. Appl. Phys. **58**, R1 (1985).